ARCHIVES OF METALLURGY

Volume 46 2001 Issue 1

ZBIGNIEW MALINOWSKI*

ANALYSIS OF TEMPERATURE FIELDS IN THE TOOLS DURING FORGING OF AXIALLY SYMMETRICAL PARTS

ANALIZA PÓL TEMPERATURY NARZĘDZI W CZASIE KUCIA ODKUWEK OSIOWOSYMETRYCZNYCH

An evaluation of the temperature distribution in tools during forging of axially symmetrical parts was performed. The finite element method was employed both for the material flow and temperature field computations. Heat generation due to plastic work and friction on the workpiece — tools contact surfaces was accounted for. Heat losses to the dies and environment were computed leading to tools temperature increase. Then, tolls cooling was modelled. The heat transfer from tools to the atmosphere, lubricant, cooling water and water sprays was accounted for. The results of the finite element modelling have demonstrated that during the forging operations the die surface temperature rises locally up to 618—630°C at the end of plastic deformation and drops to approximately 400°C after cooling. The punch surface temperature rises to 570—585°C at the end of the plastic deformation and drops to 370°C after cooling. The workpiece temperature resulting from thermal-mechanical modelling of the first operation was employed as the initial preform temperature at the second operation. The finite element modelling of the following forging operations have shown that the die temperature stabilises after 16 minutes of forging. Based on the results of computation it has been demonstrated that the water spray cooling of the punch is sufficient at the press rate of 15rpm. Further, finite element modelling of forging operations indicate that water spray cooling on the die face and water cooling on the outer die surface is needed in order to stabilise the die temperature at the values below 630°C. Temperature variation due too heating and cooling cycles take place in surface layer of the tools. The thickness of the layer ranges from 2 to 3 mm.

W artykule przedstawiono analizę pól temperatury matryc, stempli i wypychaczy w procesach kucia odkuwek osiowosymetrycznych. Zastosowano metodę elementów skończonych do obliczeń płynięcia odkształcanego metalu oraz do wyznaczenia pól temperatury. W obliczeniach pól temperatury uwzględniono ciepło odkształcenia plastycz-

* WYDZIAŁ METALURGII I INŻYNIERII MATERIAŁOWEJ, AKADEMIA GÓRNICZO-HUTNICZA, 30-059 KRAKÓW, AL. MICKIEWICZA 30

nego oraz ciepło tarcia na powierzchni styku odkształcanego materiału z narzędziami. Wzrost temperatury matryc w czasie odkształcenia plastycznego wyznaczono z bilansu ciepła przejmowanego od kutego materiału i traconego do otoczenia. Następnie modelowano chłodzenie narzędzi natryskami wodnymi na powierzchnię wykroju, chłodzenie w wyniku smarowania, straty ciepła do atmosfery oraz chłodzenie wkładki matrycowej płaszczem wodnym po zewnętrznej stronie wkładki. Wyniki obliczeń metodą elementów skończonych wykazały, że temperatura powierzchni wykroju matryc wzrasta do 618—630°C pod koniec odkształcenia plastycznego, a następnie spada do około 400°C po chłodzeniu wodnym, smarowaniu i chłodzeniu do atmosfery w czasie przerwy pomiędzy kolejnymi cyklami kucia. Temperatura powierzchni stempli wzrasta do około 570—585°C pod koniec odkształcenia plastycznego a następnie spada do około 370°C po chłodzeniu. Wyznaczone pole temperatury przedkuwki odkutej w pierwszej operacji kucia przyjęto jako początkowe pole temperatury odkształcanego materiału do modelowania zmian temperatury matryc w drugiej operacji kucia. Obliczenia przeprowadzone dla kolejnych operacji kucia wykazały, że temperatura matryc stabilizuje się po 16 minutach kucia, w przypadku prasy kujące z prędkością 16 odkuwek na minutę. Obliczenia wykazały, że zastosowanie chłodzenia powierzchni stempli natryskami wodnymi jest wystarczające do utrzymania temperatury powierzchni stempli na dopuszczalnym poziomie. W przypadku matryc konieczne jest jednak zastosowanie dodatkowego chłodzenia wkładek matrycowych płaszczem wodnym po zewnętrznej powierzchni wkładki. System taki umożliwia utrzymanie temperatury powierzchni wykroju wkładek matrycowych poniżej 630°C. Zmiany temperatury matryc, stempli i wypychaczy sięgają na głębokość od 2 do 3 mm.

1. Introduction

Prediction of the temperature rise in tools employed in forging processes can be accomplished using computer simulation of the process. The mathematical model describing the forging process consists of the two main parts: thermal and mechanical, which are coupled. Heat transfer plays an important role in forging processes where both the material flow and tools behaviour are strongly affected by the temperature field. Especially in hot forging processes where presses operate at high rates of 12 to 15 rpm. The temperature alters significantly the material properties. Thus, the dies temperature must be maintained below the maximum working temperature of the material, which was used for dies. Simultaneously, too low surface temperature of dies leads to defects of die forgings. Thus, coupled thermal-mechanical model of the die forging process, which can be used to predict dies temperature during forging, should include: determination of the material flow, increase of the temperature of the workpiece due to the work of deformation, heat transfer from the workpiece to dies, dies cooling in the air, spray and water cooling of dies, dies cooling by lubricant. The solution must starts from the initial temperature of dies and should be carried out until the dies reach the maximum working temperature. The finite element model has been developed to solve the problem. The mechanical part of the model is described in [1].

LIST OF SYMBOLS

B_d — boundary of the die
B_{da} — boundary of the die which, is in contact with the surrounding air
B_{ds} — boundary of the die which, is water spray cooled or lubricated
B_{dp} — boundary of the die which, is in contact with the punch
B_e — boundary of the pusher
B_{ea} — boundary of the pusher which, is in contact with the surrounding air
B_{ed} — boundary of the pusher which, is in contact with the die
B_{es} — boundary of the pusher which, is water spray cooled or lubricated
B_{ew} — boundary of the pusher which, is in contact with the workpiece
B_p — boundary of the punch
B_{pa} — boundary of the punch which, is in contact with the surrounding air
B_{ps} — boundary of the punch which, is water spray cooled or lubricated
B_w — boundary of the workpiece
B_{wa} — boundary of the workpiece which, is in contact with the surrounding air
B_{wat} — boundary of the die which, is water cooled
B_{wd} — boundary of the workpiece which, is in contact with the die
B_{we} — boundary of the workpiece which, is in contact with pusher
B_{wp} — boundary of the workpiece which, is in contact with the punch
c — constant equal 20 for steel
c_p — specific heat (J/kgK)
C_{ij} — heat capacity matrix
D_f — determinant of the element boundary transformation matrix
D_v — determinant of the element transformation matrix
E — Young's modulus, (MPa)
G_i — heat load vector
H' — plastic hardening modulus
K_{ij} — conductivity matrix
m — friction factor
n_r, n_z — direction cosines of the outward normal to the boundary surface
N_i — linear shape functions
q_v — rate of heat generation due to plastic work done (W/m^3)
q_a — heat transfer rate on the air cooled surface (W/m^2)
q_s — heat transfer rate on the water spray cooled or lubricated surface (W/m^2)
q_w — heat transfer rate on the water cooled surface (W/m^2)
$q_1,...q_{10}$ — heat transfer rates (W/m^2)
r, θ, z — cylindrical co-ordinate
t — temperature (°C)
T — temperature (K)
T_a — ambient temperature (K)
T_d — die temperature (K)
T_e — pusher temperature (K)
T_i — nodal temperature vector (K)
$\dot{T}_i$ — time derivatives of the nodal temperatures vector
T_p — punch temperature (K)
$\dot{T}_p$ — water spray temperature (K)
T_w — workpiece temperature (K)
T_{wo} — initial workpiece temperature (K)
α_a — heat transfer coefficient for air cooling (W/Km^2)
α_c — heat transfer coefficient under low pressure contact (W/Km^2)

α_l — heat transfer coefficient for lubricant cooling (W/Km^2)
α_p — heat transfer coefficient under plastic deformation (W/Km^2)
α_r — radiation heat transfer coefficient (W/Km^2)
α_s — heat transfer coefficient for spray cooling (W/Km^2)
α_w — heat transfer coefficient for water cooling (W/Km^2)
ε — surface emissivity
ε_s — emissivity of the system
$\dot{\bar{\varepsilon}}$ — effective rate of deformation
λ — thermal conductivity (W/mK)
λ_w — thermal conductivity of the workpiece (W/mK)
λ_d — thermal conductivity of the die (W/mK)
λ_e — thermal conductivity of the pusher (W/mK)
λ_p — thermal conductivity of the punch (W/mK)
ϱ — density (kg/m^3)
σ_p — flow stress, MPa
τ — time (s)
$\tau_a{}^a$ — air cooling time (s)
τ_d — plastic deformation time (s)
τ_e — time of the preform pushing out (s)
τ_l — time of lubricating (s)
τ_s — water spray cooling time (s)
τ_I — time of forging per one piece (s)
$\Delta\tau$ — time increment (s)

2. Heat transfer model

The distribution of the temperature in the dies and in the workpiece is determined by solving the heat conduction differential equation for the axially symmetrical problem. The scheme of the forging process is shown in figure 1. Forging is composed of four steps: plastic deformation of the workpiece τ_d, pushing out the preform τ_e, tools spray cooling τ_s, tools lubrication τ_l, tools cooling in air τ_a. Thus, the time required to forge one piece is

$$\tau_I = \tau_d + \tau_e + \tau_s + \tau_l + \tau_a \tag{1}$$

Prior to forging, the stock material is heated and its initial temperature is maintained approximately constant during forging. Tools temperatures, however, rise from the initial ones to the equilibrium temperatures which have to be determined. Thus, the solution must be carried out not for one forging cycle but as far as the tools temperatues rise. The heat conduction equation is solved successively for the workpiece, the die, the punch and the pusher. The workpiece temperature field is determined by solving the equation

$$\lambda_w\left(\frac{\partial^2 T_w}{\partial r^2}+\frac{1}{r}\frac{\partial T_w}{\partial r}\frac{\partial^2 T_w}{\partial z^2}\right)+q_v-\varrho c_p\frac{\partial T_w}{\partial \tau}=0. \tag{2}$$

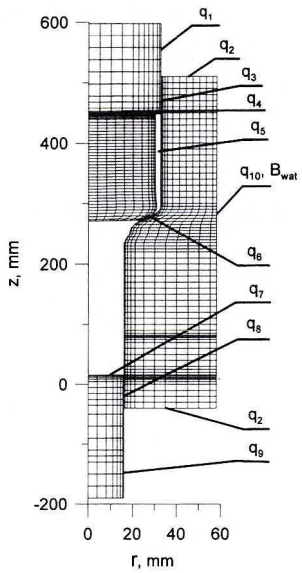

Fig. 1. Scheme of the boundary conditions and finite element discretization of the workpiece and tools used in modelling the first forging operation

The workpiece temperature field must satisfy the boundary conditions: for plastic deformation phase:

$$q_4 = -\lambda_w\left(\frac{\partial T_w}{\partial r}n_r + \frac{\partial T_w}{\partial z}n_z\right) = \alpha_p(T_w - T_p)\,\text{at}\,z = B_{wp} \tag{3}$$

$$q_5 = -\lambda_w\left(\frac{\partial T_w}{\partial r}n_r + \frac{\partial T_w}{\partial z}n_z\right) = \alpha_r(T_w - T_d)\,\text{at}\,r = B_{wd} \tag{4}$$

$$q_6 = -\lambda_w\left(\frac{\partial T_w}{\partial r}n_r + \frac{\partial T_w}{\partial z}n_z\right) = \alpha_p(T_w - T_d)\,\text{at}\,r = B_{wd} \tag{5}$$

$$q_7 = -\lambda_w\left(\frac{\partial T_w}{\partial r}n_r + \frac{\partial T_w}{\partial z}n_z\right) = \alpha_r(T_w - T_e)\,\text{at}\,z = B_{we}, \tag{6}$$

for pushing out phase:

$$q_e = -\lambda_w\left(\frac{\partial T_w}{\partial r}n_r + \frac{\partial T_w}{\partial z}n_z\right) = \alpha_c(T_w - T_e)\,\text{on}\,B_{we} \tag{7}$$

$$q_r = -\lambda_w\left(\frac{\partial T_w}{\partial r}n_r + \frac{\partial T_w}{\partial z}n_z\right) = \alpha_r(T_w - T_i)\,\text{on}\,B_{wr} \tag{8}$$

$$q_a = -\lambda_w\left(\frac{\partial T_w}{\partial r}n_r + \frac{\partial T_w}{\partial z}n_z\right) = \alpha_a(T_w - T_a)\,\text{on}\,B_{wa} \tag{9}$$

For air cooling phase the heat transfer rate q_a is specified on the workpiece surface B_w. Once the stock material is heated to the approximately constant temperature. The following initial condition is assumed for each sample

$$T_w(r, z, \tau = 0) = T_{wo}. \tag{10}$$

The rate of internal heat generation q_v due to plastic work is defined as

$$q_v = \sigma_p \dot{\bar{\varepsilon}} \left(1 - \frac{cH'}{E}\right), \tag{11}$$

where c is a material parameter, $c = 20$ for steel [2]. The radiation heat transfer takes place between the workpiece, the die, the punch and the pusher an surfaces which are not in contact. In this case the heat transfer coefficient is

$$\alpha_r = \varepsilon_s \cdot 5{,}6693 \cdot 10^{-8} \frac{T_w^4 - T_i^4}{T_w - T_i}, \tag{12}$$

where T_i represents the temperature of a body, which exchange heat with the workpiece. The emissivity of the system ε_s is given by

$$\varepsilon_s = \frac{1}{\frac{1}{\varepsilon_w} + \frac{1}{\varepsilon_i} - 1}. \tag{13}$$

Emissivities of surfaces taking part in the exchange process may be determined from [3]

$$\varepsilon = 1.1 + \frac{T-273}{1000}\left(0.125\frac{T-273}{1000} - 0.38\right). \tag{14}$$

Making the substitutions: $T = T_w$, $T = T_d$, $T = T_p$, $T = T_e$ emissivities of the workpiece e_w, the die ε_d, the punch ε_p and the pusher ε_e can be calculated, respectively. Part of the deformed material surface is in contact with the tools. In this case the heat transfer coefficient may be evaluated from

$$\alpha_p = 20438 - 5936\frac{T_w - 273}{1000} + 16943\left(\frac{T_w - 273}{1000}\right)^2 \quad \text{for } T_w < 973\,\text{K} \tag{15}$$

$$\alpha_p = 115566 - 190554\frac{T_w - 273}{1000} + 85068\left(\frac{T_w - 273}{1000}\right)^2 \quad \text{for } T_w > 973\,\text{K}. \tag{16}$$

For pushing out phase part of the preform surface is in contact with the tools under low normal pressure. In this case the heat transfer coefficient may be evaluated from

$$\alpha_c = 2150 - 4114\frac{T_w - 273}{1000} + 13243\left(\frac{T_w - 273}{1000}\right)^2 \quad \text{for } T_w < 973\,\text{K} \tag{17}$$

$$\alpha_c = -3300 + 18858\frac{T_w - 273}{1000} + 8418\left(\frac{T_w - 273}{1000}\right)^2 \quad \text{for } T_w > 973\,\text{K}. \tag{18}$$

Equations for the heat transfer coefficient under high and low pressures have been developed based on data published in [4]. The preform looses heat by natural convection and radiation to the atmosphere. To account for these on a boundary surface which, is in contact with the air, the heat transfer rate has to be determined. The heat exchange with the surrounding air is calculated by means of the combined free convection and radiation. Measurements of temperatures during cooling of the workpiece in the atmosphere and numerical tests performed in [4] have given the heat transfer coefficient on cylindrical surfaces cooled in air

$$\alpha_a = \left(1.2 - 0.52\frac{T_w - 273}{1000}\right) \cdot 5.6693 \cdot 10^{-8}\frac{T_w^4 - T_a^4}{T_w - T_a}. \tag{19}$$

The next step is a determination of the tools temperatures. It can be accomplished by solving the deferential equation

$$\lambda\left(\frac{\partial^2 T}{\partial r^2} + \frac{1}{r}\frac{\partial T}{\partial r}\frac{\partial^2 T}{\partial z^2}\right) - \varrho c_p \frac{\partial T}{\partial \tau} = 0. \tag{20}$$

Making the substitutions: $T = T_d$, $T = T_p$, $T = T_e$ temperature fields for the die, the punch and the pusher can be calculated, respectively. The tools temperature fields must satisfy the boundary conditions for plastic deformation stage τ_d, pushing out the preform τ_e, tools spray cooling τ_s, tools lubrication τ_1, and tools cooling in air τ_a. For plastic deformation stage the boundary conditions, which must satisfy the die temperature field, are given by:

$$q_2 = -\lambda_d\left(\frac{\partial T_d}{\partial r}n_r + \frac{\partial T_d}{\partial z}n_z\right) = \alpha_a(T_d - T_a)\,\text{at}\,z = B_{da} \tag{21}$$

$$q_3 = -\lambda_d\left(\frac{\partial T_d}{\partial r}n_r + \frac{\partial T_d}{\partial z}n_z\right) = \alpha_c(T_d - T_p)\,\text{at}\,r = B_{dp} \tag{22}$$

$$q_5 = -\lambda_d\left(\frac{\partial T_d}{\partial r}n_r + \frac{\partial T_d}{\partial z}n_z\right) = \alpha_r(T_d - T_p)\,\text{at}\,r = B_{wd} \tag{23}$$

$$q_6 = -\lambda_d\left(\frac{\partial T_d}{\partial r}n_r + \frac{\partial T_d}{\partial z}n_z\right) = \alpha_p(T_d - T_w)\,\text{at}\,r = B_{wd} \tag{24}$$

$$q_8 = -\lambda_d\left(\frac{\partial T_d}{\partial r}n_r + \frac{\partial T_d}{\partial z}n_z\right) = \alpha_c(T_d - T_e)\,\text{at}\,r = B_{ed}. \tag{25}$$

For pushing out phase the die temperature field must satisfy boundary condition given by the heat transfer rates: q_2, q_3, q_5, q_8. Once the preform i pushed out of the die, the water spray cooling phase starts. The die temperature field must satisfy the boundary condition defined by the heat transfer rate q_2, on the boundary surface which is in contact with air. On the die face B_{ds}, which is water spray cooled the boundary condition is specified

$$q_s = -\lambda_d\left(\frac{\partial T_d}{\partial r}n_r+\frac{\partial T_d}{\partial z}n_z\right)=\alpha_s(T_d-T_s)\text{ on }B_{ds}. \tag{26}$$

When water is applied to the hot steel surface, the rate of heat transfer is controlled by the thermal properties of the steel, the water and the interface. The interface heat flow is controlled by the surface total heat transfer coefficient α_s, and the difference in temperature between the steel surface and the applied coolant. The total heat transfer coefficient includes both convective and radiative components. In the case of the water spray cooling, the water flux rate is an additional parameter, which affects the heat transfer coefficient. Laboratory measurements were carried out in [5] to determine the heat transfer coefficient, leading to:

$$\alpha_s=3.15\times10^9\dot{w}^{0.616}\left[700+\frac{t-700}{\exp(0.1t-70)+1}\right]^{-2.455}\left[1-\frac{1}{\exp(0.025t-6.25)+1}\right]. \tag{27}$$

This equation is valid for the tool surface temperatures t from 150°C to at least 900°C and the water flux rate from 0.16 to 62 $\text{ls}^{-1}\text{m}^{-2}$. After water spray cooling the die is lubricated. Cooling of tools while lubricating is estimated by a constant heat transfer coefficient [6]

$$\alpha_l = 1500\,\text{W/m}^2\text{K}\ \text{ on }\ B_{ds}. \tag{28}$$

The last stage is air cooling of the die and the heat transfer coefficient is calculated from equation (19). The die is water cooled during the process of forging and the heat transfer rate q_{10} is calculated using the heat transfer coefficient α_w shown in figure 2 [5].

The punch temperature field must satisfy boundary conditions similar to those described for the die. During plastic deformation stage boundary conditions for the punch are given by

$$q_1 = -\lambda_p\left(\frac{\partial T_p}{\partial r}n_r+\frac{\partial T_p}{\partial z}n_z\right)=\alpha_a(T_p-T_a)\,\text{at}\,r\ =B_{pa} \tag{29}$$

$$q_3 = -\lambda_p\left(\frac{\partial T_p}{\partial r}n_r+\frac{\partial T_p}{\partial z}n_z\right)=\alpha_c(T_p-T_d)\,\text{at}\,r\ =B_{dp} \tag{30}$$

$$q_4 = -\lambda_p\left(\frac{\partial T_p}{\partial r}n_r+\frac{\partial T_p}{\partial z}n_z\right)=\alpha_p(T_p-T_w)\,\text{at}\,r\ =B_{wp} \tag{31}$$

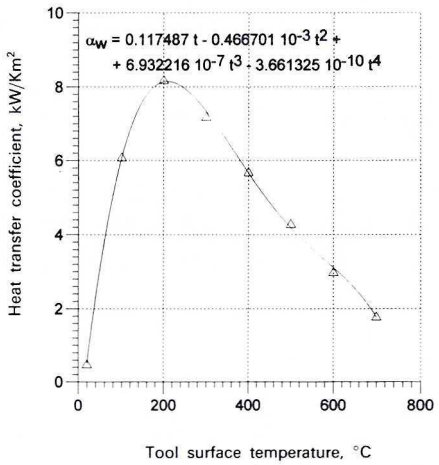

Fig. 2. Variation of the heat transfer coefficient versus the tool surface temperature during water cooling

For pushing out phase the punch temperature field must satisfy boundary conditions given by the heat transfer rate q_1 on the punch surface B_p. Once the preform is pushed out of the die, the water spray cooling phase starts. The punch temperature field must satisfy the boundary condition defined by the heat transfer rate q_2 on the boundary surface, which is in contact with air. On the punch face B_{ps} which is water spray cooled, the heat transfer coefficient given by equation (27) is specified. Cooling of punch while lubricating is estimated by a constant heat transfer coefficient given by equation (28). The last stage is air cooling of the punch and the heat transfer coefficient is calculated from equation (19).

The pusher temperature field must satisfy boundary conditions similar to whose described for the punch. During plastic deformation stage boundary conditions for the pusher are given by

$$q_7 = -\lambda_e\left(\frac{\partial T_e}{\partial r}n_r + \frac{\partial T_e}{\partial z}n_z\right) = \alpha_r(T_e - T_w)\,\text{at}\,z = B_{ew} \tag{32}$$

$$q_8 = -\lambda_e\left(\frac{\partial T_e}{\partial r}n_r + \frac{\partial T_e}{\partial z}n_z\right) = \alpha_c(T_e - T_d)\,\text{at}\,r = B_{ed} \tag{33}$$

$$q_9 = -\lambda_e\left(\frac{\partial T_e}{\partial r}n_r + \frac{\partial T_e}{\partial z}n_z\right) = \alpha_a(T_e - T_a)\,\text{at}\,z = B_{ea}\,. \tag{34}$$

For pushing out phase the pusher temperature field must satisfy boundary conditions given by equations (32), (33) and (34). The contact surfaces B_{ed} and B_{ea} are calculated taking into account actual location of the pusher. Once the preform is pushed out of the die, the pusher is water spray cooled and the pusher temperature field must satisfy the boundary condition defined by the heat transfer coefficient

given by equation (27) on the boundary surface B_{es}. Cooling of the pusher while lubricating is estimated by a constant heat transfer coefficient given by equation (28). The last stage is air cooling of the pusher and the heat transfer coefficient is calculated from equation (19).

Tools temperature changes during forging. The tools temperature fields computation starts from the initial temperature equal to ambient temperature. It makes possible to compute tools temperature field at the end of time $\tau = \tau_I$, which is necessary to forge one piece. Next the computed temperature filed

$$T(r, z) = T_{tool}(r, z, \tau = k \cdot \tau_I) \tag{35}$$

is taken as the initial tool temperature field for computation of the heat transfer during plastic deformation of the workpiece $k+1$, pushing out the preform, tools spray cooling, tools lubricating, and tools cooling in air. In equation (35) k represents number of forgings already forged.

The finite element discretization of the heat conduction equation is accomplished in a way typical for the finite element method. An application of the weighted residuals technique to the heat transfer equation leads to the set of partial differential equations

$$K_{ij}(\tau)T_j(\tau)+C_{ij}(\tau)\dot{T}_j(\tau) = G_i(\tau). \tag{36}$$

Assuming the linear temperature approximation over the period of time $\Delta\tau$ and applying Galerkin method equation (36) takes the form

$$A_{ij}(\tau)T_j(\tau+\Delta\tau) = B_i(\tau), \tag{37}$$

where

$$A_{ij}(\tau) = \frac{1}{3}K_{ij}(\tau)+\frac{1}{2\Delta\tau}C_{ij}(\tau) \tag{38}$$

$$B_i(\tau) = \left[-\frac{1}{6}K_{ij}(\tau)+\frac{1}{2\Delta\tau}C_{ij}(\tau)\right]T_i(\tau)-G_i(\tau)\left[\frac{1}{2}+\frac{1}{3}\frac{\Delta\tau}{\Delta\tau_0}\right]+\frac{1}{3}\frac{\Delta\tau}{\Delta\tau_0}G_i(\tau-\Delta\tau). \tag{39}$$

For one element vector G_i and matrixes C_{ij}, K_{ij} may be written as

$$G_i = \sum_{s=1}^{4} L^s \sum_{k=1}^{2} N_i \alpha^k T_a^k D_f^k r^k \tag{40}$$

$$C_{ij} \sum_{k=1}^{4} N_i N_j \varrho^k c_p^k D_v^k r^k \tag{41}$$

$$K_{ij} = \sum_{k=1}^{4} \lambda^k \left(\frac{\partial N_i}{\partial r}\frac{\partial N_j}{\partial r}+\frac{\partial N_i}{\partial z}\frac{\partial N_j}{\partial z}\right) D_v^k r^k + \sum_{s=1}^{4} L^s \sum_{k=1}^{2} N_i N_j \alpha^k D_f^k r^k, \tag{42}$$

where L^s is an integer equal to 1 for the side of an element where boundary conditions are specified, otherwise L^s is equal to zero. An integer s indicates a side of an element and an integer k indicates the number of G a u s s' point.
Derivatives of the linear shape functions with respect to global co-ordinates are given by:

$$\frac{\partial N_k}{\partial r} = J^{-1}\frac{\partial N_k}{\partial \xi_1}$$
$$\frac{\partial N_k}{\partial z} = J^{-1}\frac{\partial N_k}{\partial \xi_2}. \tag{43}$$

Determinant of the transformation matrix which relates global to local co-ordinates may be written as

$$D_v = \det \begin{bmatrix} \frac{\partial r}{\partial \xi_1} & \frac{\partial r}{\partial \xi_2} \\ \frac{\partial z}{\partial \xi_1} & \frac{\partial z}{\partial \xi_2} \end{bmatrix}. \tag{44}$$

In one dimensional case on the boundary of an element determinant of the co-ordinates transformation is given by

$$D_f = \frac{\partial l}{\partial \xi_1} = \sum_{k=1}^{2} \frac{\partial N_k}{\partial \xi_1} l^k. \tag{45}$$

The inverse transformation matrix has the form

$$J_{ki}^{-1} = \frac{1}{D_v} \begin{bmatrix} \frac{\partial z}{\partial \xi_2} & -\frac{\partial r}{\partial \xi_2} \\ -\frac{\partial z}{\partial \xi_1} & \frac{\partial r}{\partial \xi_1} \end{bmatrix}. \tag{46}$$

Linear shape functions have been used in finite element model

$$N_k = \frac{1}{4}\left(1+\xi_1\xi_1^k\right)\left(1+\xi_2\xi_2^k\right). \tag{47}$$

Derivatives of global co-ordinates with respect to local co-ordinates may be written as

$$\frac{\partial r}{\partial \xi_1} = \frac{1}{4}\sum_{k=1}^{4} \xi_1^k \left(1 + \xi_2 \xi_2^k\right) r^k$$

$$\frac{\partial r}{\partial \xi_2} = \frac{1}{4}\sum_{k=1}^{4} \xi_2^k \left(1 + \xi_1 \xi_1^k\right) r^k \tag{48}$$

$$\frac{\partial z}{\partial \xi_1} = \frac{1}{4}\sum_{k=1}^{4} \xi_1^k \left(1 + \xi_2 \xi_2^k\right) z^k$$

$$\frac{\partial z}{\partial \xi_2} = \frac{1}{4}\sum_{k=1}^{4} \xi_2^k \left(1 + \xi_1 \xi_1^k\right) z^k \tag{49}$$

$$\frac{\partial l}{\partial \xi_1} = \frac{1}{2}\sum_{k=1}^{2} \xi_1^k \, l. \tag{50}$$

Local co-ordinates of an element are denoted as ξ_i^k, r^k, z^k denote global co-ordinates of an element, l represents length of an element side. In the developed finite element model the change of the boundary conditions over time increment $\Delta\tau$ is introduced in $B(\tau)$. It stabilises the solution for variable time increments and variable boundary conditions. It makes possible to use longer time increments in finite element computations.

3. Results and discussion

The part selected for thermal-mechanical modelling is forged in two operations. In order to determine temperature changes in tools and in workpiece during forging and cooling, the computations have been performed for both operations.

3.1. First operation

In the first operations a billet of 30.16 mm in diameter and 175 mm in height is forged in dies whose finite element discretization is shown in figure 1. The initial temperature of the workpiece was assumed equal to 904°C and the initial temperature of the dies was set to 50°C. The flow stress of the workpiece material was calculated from the empirical equation developed by S h i d a [7]. Friction at the workpiece — tools interface was modelled using friction factor $m = 0.1$. It was assumed that the press works at the rate of 15 rpm. The vertical velocity of the punch was calculated from the speed diagram, which has given the plastic deformation time of $\tau_d = 0.4$s. During forging the workpiece is deformed plastically and the deforma-

tion process was modelled using an incremental finite element formulation [1]. After each time increment the punch was moved down by 1 mm. Having determined the material flow, the workpiece — tools contact surfaces B_{wd}, B_{wp}, B_{we}, ware updated after each time increment, and new temperature fields in the tools and in the workpiece ware computed. Further, it was assumed that the die is water cooled during the process of forging at the boundary B_{wat}, as depicted in figure 1.

Forging at the rate of 15 rpm results in a significant temperature rise in the tools. Stationary conditions have been reached after 6 minutes of forging. The detailed maps of the tools temperatures are presented in figures 3, 4 and 5 for the die, the

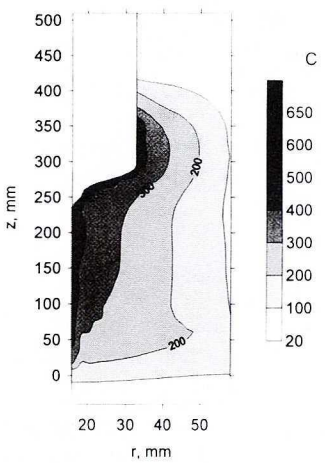

Fig. 3. The temperature field of the die at the end of plastic deformation of the workpiece, computed for the first operation

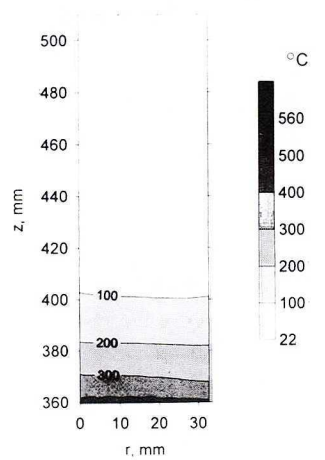

Fig. 4. The punch temperature field at the end of plastic deformation of the workpiece, computed for the first operation

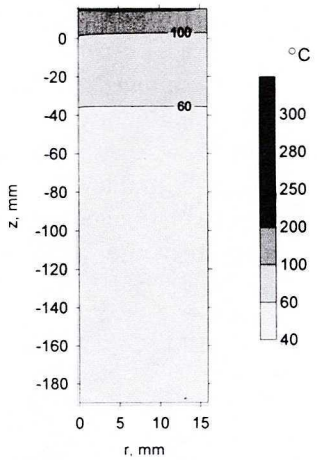

Fig. 5. The pusher temperature field at the end of plastic deformation of the workpiece computed for the first operation

punch and the pusher, respectively. The die has the highest face temperature of 618°C at a conical part (figure 6). Die segments above and below the conical part have lower face temperatures. The punch has the maximum face temperature of 570°C (figure 7) and the pusher of 340°C (figure 5).

After forging the die and the pusher undergo further heat exchange due to heating and cooling while a preform is removed from the die. That period of time takes 1s of the total time of 4s available at the press speed of 15rpm. The heat exchange was computed using α_a, α_c, α_r heat transfer coefficients. Then, the die and the pusher are cooled for 1s and lubricated for 0.2s. The heat exchange between tools and water and lubricant sprays was computed using the heat transfer coefficients α_s, α_l. The spray flux rate of 4 $1s^{-1}m^{-2}$ was assumed in computations. For the rest of time $\tau_a = 1.4s$

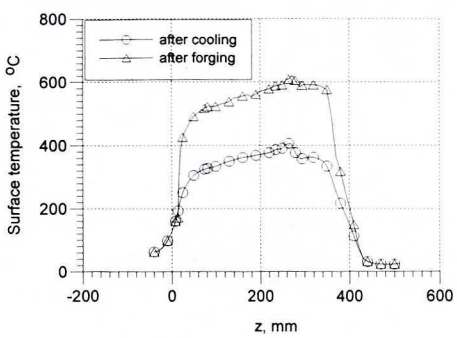

Fig. 6. The die face temperatures at the end of plastic deformation of the work piece and after cooling, computed for the first operation

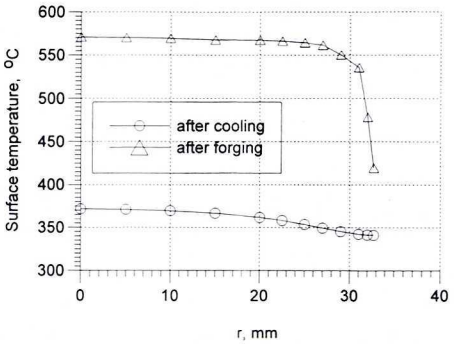

Fig. 7. The punch face temperatures at the end of plastic deformation of the workpiece and after cooling, computed for the first operation

the die and the pusher ware air cooled and the heat exchange at the tools — air interfaces was computed using the heat transfer coefficient α_a.

The punch is water spray cooled for 0.4s, lubricated for 0.2s and air cooled for 3s. The heat transfer coefficients were calculated in the same way as described for the die. The water and water spray temperatures of 20°C, the air temperature of 20°C and the lubricant temperature of 30°C were assumed in computations.

After cooling the die has the highest face temperature of 406°C at the conical part, see figure 6. The die segments below and above the conical part have the maximum face temperature below 350°C. The punch has the maximum surface temperature of 370°C (figure 7) and this temperature for the pusher is 175°C. The applied cooling system involving water sprays results in significant drops in tools temperatures at the

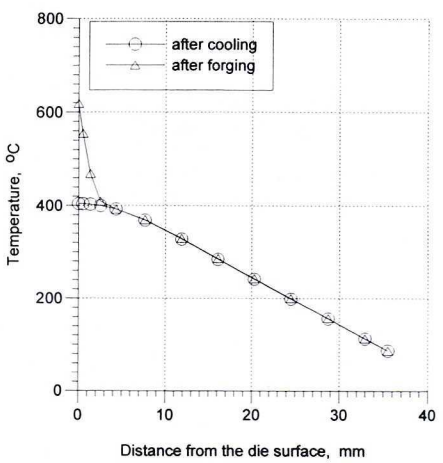

Fig. 8. Temperature variation versus the distance from the die surface at $z = 270$ cross-section at the end of plastic deformation of the workpiece and after cooling, computed for the first operation

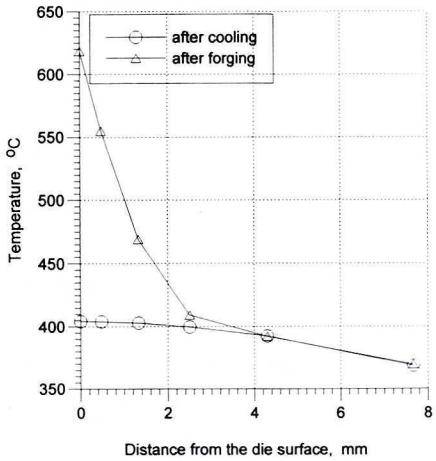

Fig. 9. Local temperature variation versus the distance from the die surface at the end of plastic deformation of the workpiece and after cooling, computed for the first operation

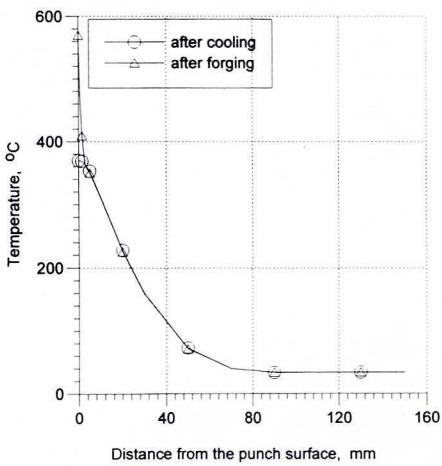

Fig. 10. Temperature variation versus the distance from the punch surface at $r = 0$ cross-section at the end of plastic deformation of the workpiece and after cooling, computed for the first operation

surface layer. In figures 8, 9, 10 and 11 the temperature variations in the die and punch surface layers caused by cooling are presented. The temperature drops by about 200°C. The temperature shock caused by cooling vanishes at the depths of 3 mm below the tools surfaces, as shown in figures 9 and 11.

In the first operation, the workpiece temperature drops at the outer surface to the minimum value of 810°C. Below the surface at the depth of about 5 mm the material temperature is close to the initial value of 904°C prescribed for the first operation.

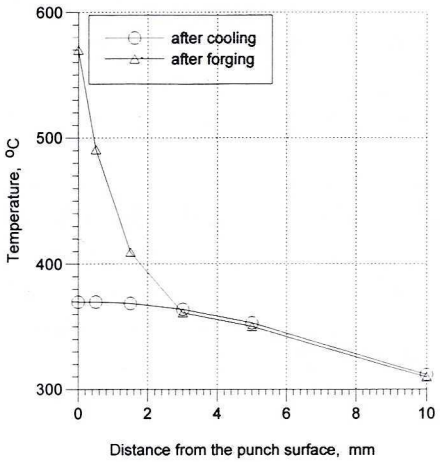

Fig. 11. Local temperature variation versus the distance from the punch surface at the end of plastic deformation of the workpiece and after cooling, computed for the first operation

3.2. Second operation

In the second operation, the preform is forged in dies whose finite element discretization is shown in figure 12. The initial temperature of the preform for the second operation was taken from the results obtained for the first operation. The

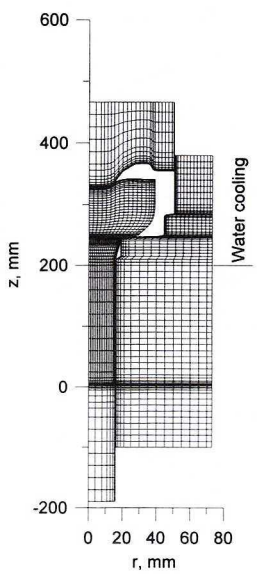

Fig. 12. Scheme of the finite element discretization of the workpiece and tools used in modelling the second forging operation

initial temperature of the dies was set to 30°C. The deformation process was modelled in the same way as described for the first operation. The vertical velocity of the pusher was calculated from the speed diagram, assuming that the press works at the rate of 15rpm. It has given the plastic deformation time of 0.3s. Two variants of cooling have been studied with and without water cooling system, figure 12.

Stationary conditions have been reached after 16 minutes of forging, if no water cooling is used on the outer surface of the die. The average temperature of the die versus number of forgings forged is shown in figure 13.

In figures 14 and 15 temperature fields for the die and the pusher are presented at the end of plastic deformation stage. The die has the face temperature ranging from 687°C to 170°C. The punch has the maximum face temperature of 585°C and the

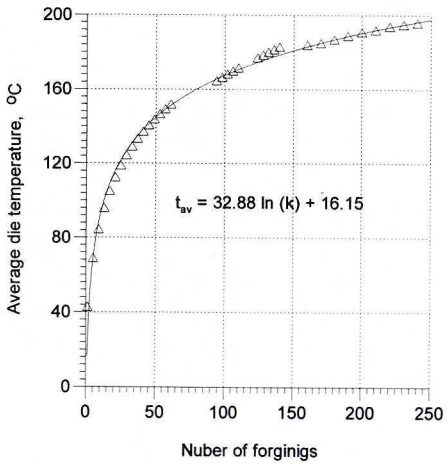

Fig. 13. Average die temperature versus number of forgings forged

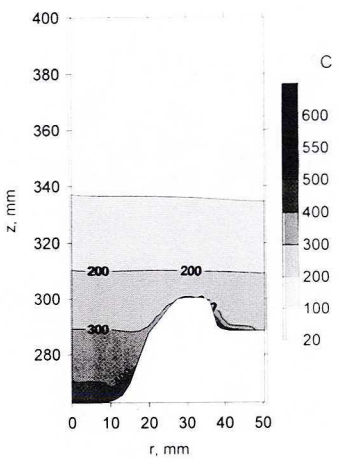

Fig. 14. The punch temperature field at the end of plastic deformation of the workpiece, computed for the second operation

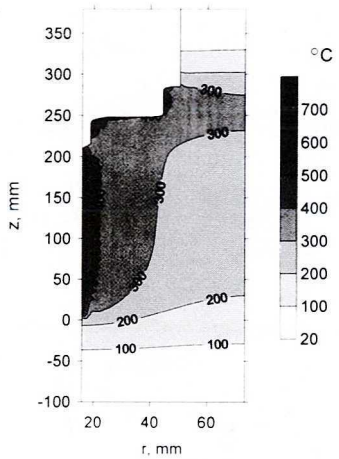

Fig. 15. The temprature field of the die at the end of forging computed for the second operation

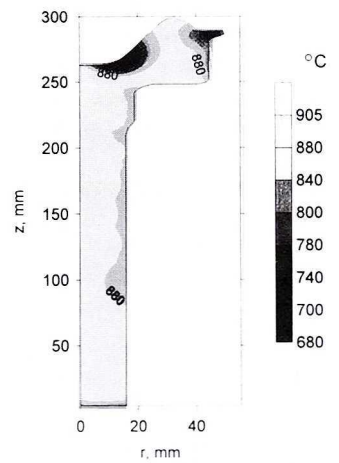

Fig. 16. The workpiece temperature at the end of second operation

temperature of the pusher is 316°C. In the second operation the workpiece temperature has dropped at the surface of contact with the punch to the minimum value of 680°C, figure 16. At the axis of symmetry the workpiece temperature ranges from 850°C to 900°C.

After forging the die and the pusher undergo further heat exchange due to heating and cooling while a forged part is removed from the die. That period of time takes 1s of the total time of 4s available at the press speed of 15rpm. Next, the die and the pusher are water spray cooled for 1s and lubricated for 0.2s. The water spray flux rate of 4 $1s^{-1}m^{-2}$ was assumed in computations. During the rest of time $\tau_a = 1.5s$ the die and the pusher are air cooled. The punch is water spray cooled for 0.4s, lubricated for 0.2s and air cooled for 3.1s. The heat transfer coefficients were

calculated in the same way as described in the first operation. The water spray temperature of 20°C, the air temperature of 20°C and the lubricant temperature of 30°C were assumed in computations.

In figures 17 and 18 temperature fields for the die and the punch are presented at the end of cooling cycles. After cooling the die has the highest face temperature of 465°C. The punch has the maximum face temperature of 370°C and the pusher of 290°C.

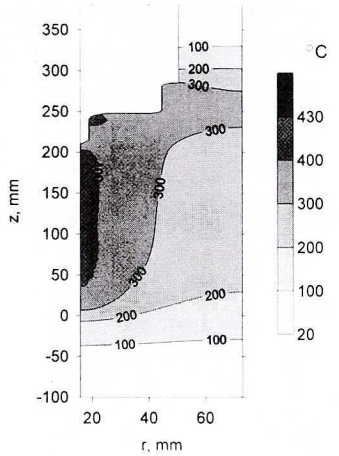

Fig. 17. The die temperature field after cooling computed for the second operation

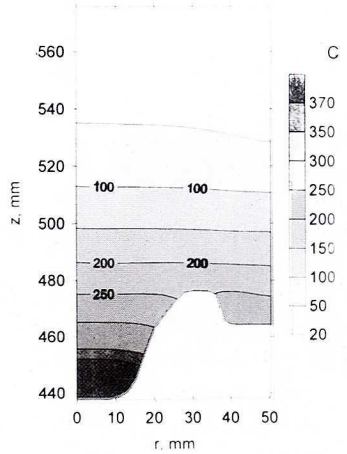

Fig. 18. The punch temperature field after cooling computed for the second operation

In figure 19 the temperature variations at the punch face after forging and cooling are presented. Water spray and lubricant cooling has lowered the punch temperature at the surface layer to the range of 370°C to 290°C. In figure 20 temperature

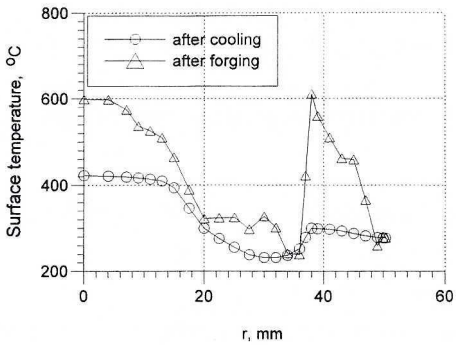

Fig. 19. The punch face temperatures at the end of forging and after cooling, computed for the second operation

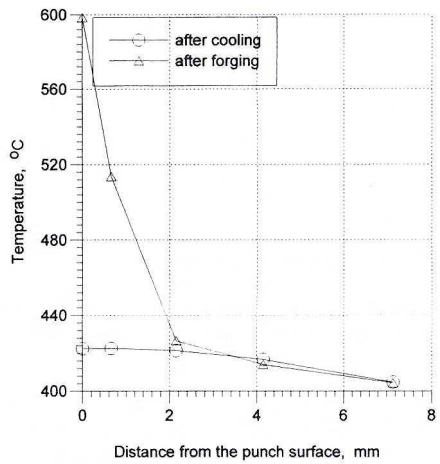

Fig. 20. Local temperature variation versus the distance from the punch surface at the end of forging and after cooling, computed for the second operation

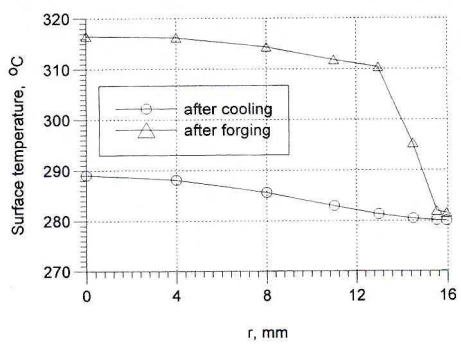

Fig. 21. The pusher surface temperatures at the end of forging and after cooling, computed for the second operation

variation in the direction normal to the punch surface are presented. The temperature changes caused by heating and cooling are localised in 2mm surface layer. The punch temperature tends to values commonly used in forging plants. The temperature variations after forging and cooling on the pusher surface are shown in figure 21. In figure 22 pusher temperature changes in the direction normal to the pusher surface are shown. The temperature drops of about 30°C. Temperature changes are localised in 2 mm surface layer.

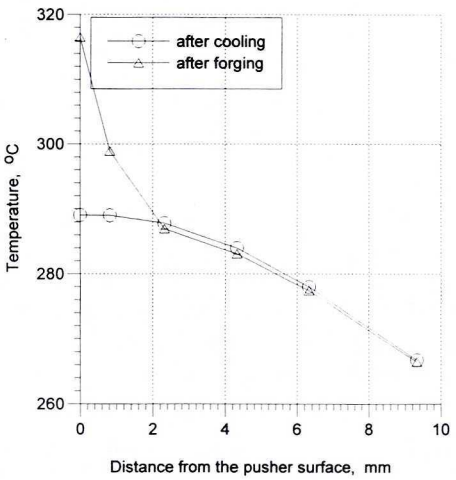

Fig. 22. Local temperature variation versus the distance from the pusher surface at the end of forging and after cooling, computed for the second operation

In case of the die results are different. In figure 23 the temperature variations at the die face after forging and cooling are shown. Due too cooling the temperature has dropped by about 200°C. The temperature shock caused by spray cooling vanishes at the depths of 3 mm below the die surface. In figures 24 and 25 variation

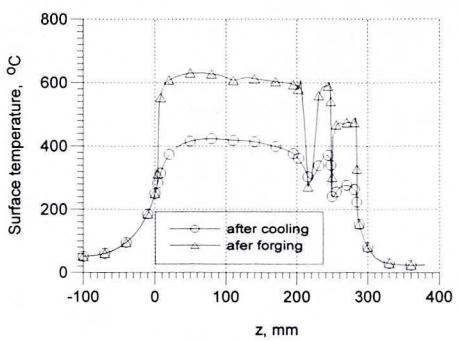

Fig. 23. The die face temperatures at the end of forging and after cooling, computed for the second operation without water cooling

of the die temperature versus the distance from the die face are plotted for $z = 235$ mm cross-section.

In order to investigate the influence of water cooling of the outer surface of the die on its temperature, additional computations were performed. It was assumed that the die has water cooling system from the top of die to the depth of $z = 200$ mm. In figures 26 and 27 variation of the die temperature versus the distance from the die face are plotted for $z = 235$ mm cross-section. With water cooling the die has the highest face temperature of 630°C, see figure 28. The water cooling on the outer die surface has lowered the die temperature at the surface layer in the cooling region of about 50°C to the values below 600°C.

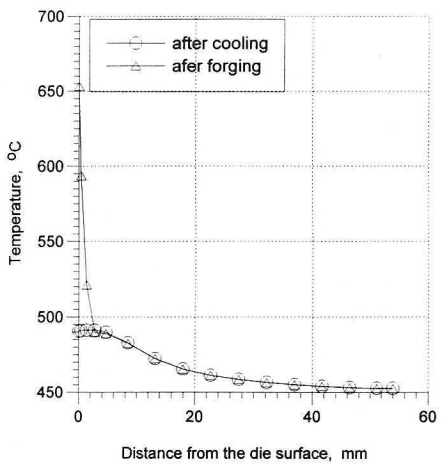

Fig. 24. Temperature variation versus the distance from the die surface at $z = 235$ cross-section at the end of forging and after cooling cycles computed for the second operation without addtitional water cooling

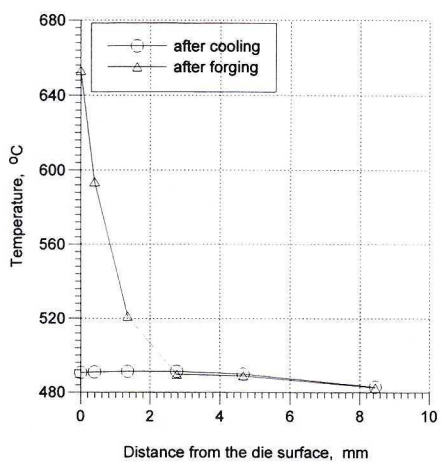

Fig. 25. Local temperature variation versus the distance from the die surface at the end of forging and after cooling, computed for the second operation without additional water cooling

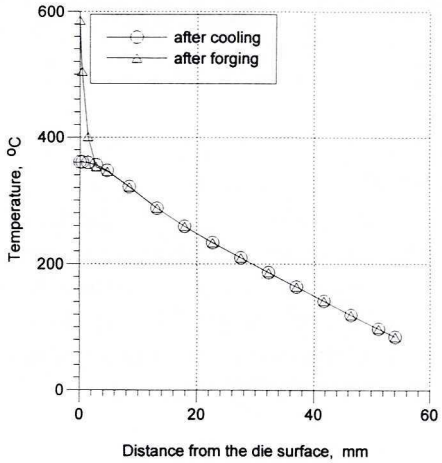

Fig. 26. Temperature variation versus the distance from the die surface at $z = 235$ cross-section at the end of forging and after cooling cycles computed for the second operation with additional water cooling

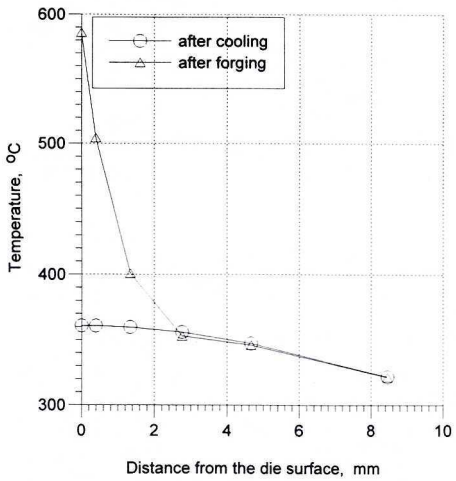

Fig. 27. Local temperature variation versus the distance from the die surface at the end of forging and after cooling, computed for the second operation with additional water cooling

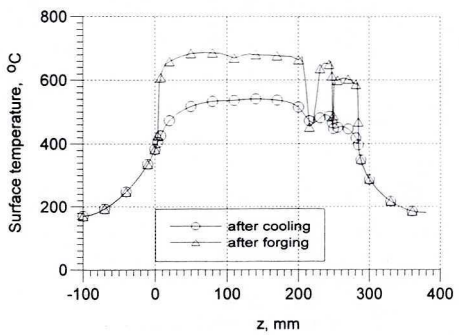

Fig. 28. The die face temperatures at the end of forging and after cooling, computed for the second operation with additional water cooling

4. Conclusions

The thermal-mechanical finite element modelling of tools heating and cooling during forging at the press rate of 15rpm were performed. The computation were carried out with the objective to determine the tools and workpiece temperature fields resulting from the forging process. Heat generation due to plastic work and friction on the workpiece — tools contact surfaces was accounted for. Heat losses of the workpiece to the tools and environment were computed leading to tools temperature increase. Simultaneously, the tools temperatures fields during heating and cooling cycles were computed. The heat losses from tools to the atmosphere, lubricant, cooling water and water sprays were accounted for.

The computations performed for the first operation have shown that the punch temperature at the surface of contact with the workpiece has the maximum value below 570°C at the end of plastic deformation and below 370°C after cooling. The die temperature at the surface of contact with the workpiece has stabilised at the value below 618°C at the end of plastic deformation and has dropped to the values below 406°C after cooling. The pusher temperature at the surface of contact with the workpiece has the maximum values below 340°C at the end of loading and below 175°C after cooling. The water spray cooling of the die face and water cooling of the outer surface of the die is sufficient for the first forging operation.

In the case of second operation the die temperature has stabilised after 16 minutes of forging. The punch temperature at the surface of contact with the workpiece has the maxim values below 585°C at the end of plastic deformation and below 370°C after cooling. The pusher temperature at the surface of contact with the workpiece has the maxim value below 316°C at the end of loading and below 290°C after cooling. The die temperature at the surface of contact with the workpiece has risen to 687°C at the end of forging and has dropped to 465°C after cooling. Implementation of the water cooling in the upper segment of the die has stabilised the die surface temperature at the maximum values below 630°C at the end of plastic deformation.

REFERENCES

[1] Z. Malinowski, Prognozowanie pól naprężeń metodą elementów skończonych w materiałach poddawanych dużym odkształceniom plastycznym. Rozprawy Monografie, Nr 13, Wydawnictwa AGH, Kraków 1994.

[2] A. T. Zehnder, A model for the heating due to plastic work, Mechanics Research Communications **18,** 23—28 (1991).

[3] C. Devadas, I. V. Samarasekera, Heat transfer during hot rolling of steel strip, Ironmaking and Steelmaking **13,** 311—321 (1986).

[4] Z. Malinowski, J. G. Lenard, M. E. Davies, A study of the heat-transfer coefficient as a function of temperature and pressure, J. Mat. Proc. Tech. **41,** 125—142 (1994).

[5] P. D. Hodgson, K. M. Browne, D. C. Collinson, T. T. Pham, R. K. Gibbs, A mathematical model to simulate the thermo-mechanical processing of steel, Proc. 3rd Int. Seminar of the International Federation for Heat Treatment and surface Engineering, 1991, Melbourne, pp. 139—159.
[6] T. Senkara, Obliczenia cieplne pieców grzewczych w hutnictwie, Wydawnictwo Śląsk 1981.
[7] C. A. F. Suzuki, Studies on the flow stress of metal. Report, The University of Tokyo **18,** 139, 145 (1968).

Financial assistance of Polish Committee for Scientific Research (KBN) is greatly acknowledged. Faculty of Metallurgy and Materials Science, University of Mining and Metallurgy, project No 11.11.110.114

REVIEWED BY: PROF. DR HAB. INŻ. MACIEJ PIETRZYK

Received: 2 December 2000.